© 2023 Institute of Theoretical Physics CAS, Chinese Physical Society and IOP Publishing Printed in China and the UK

Commun. Theor. Phys. **75** (2023) 125402 (8pp) https://doi.org/10.1088/1572-9494/ad0029

Energy in critical collapse

Yu Hu[1], Jun-Qi Guo[2], Junbin Li[3], Cheng-Gang Shao[1,*] and Hongsheng Zhang[2]

[1] MOE Key Laboratory of Fundamental Physical Quantities Measurement, Hubei Key Laboratory of Gravitation and Quantum Physics, PGMF, and School of Physics, Huazhong University of Science and Technology, Wuhan 430074, Hubei, China
[2] School of Physics and Technology, University of Jinan, Jinan 250022, Shandong, China
[3] Department of Mathematics, Sun Yat-sen University, Guangzhou 510275, Guangdong, China

E-mail: yuhu@hust.edu.cn, sps_guojq@ujn.edu.cn, lijunbin@mail.sysu.edu.cn, cgshao@hust.edu.cn and sps_zhanghs@ujn.edu.cn

Received 26 April 2023, revised 2 October 2023
Accepted for publication 5 October 2023
Published 23 November 2023

Abstract

We study the energy issue in critical collapse. It is found that in critical collapse, the contribution from the material energy is greater than that from the gravitational energy. The quantity m/r plays an important role in identifying the formation of an apparent horizon in gravitational collapse, where m is the Misner–Sharp mass and r is the areal radius. We observe that in critical collapse, the maximum value of m/r fluctuates between $2/15$ and $4/15$. This denotes a large gap between critical collapse and black hole formation for which the criterion is $m/r = 1/2$.

Keywords: quasi-local energy, critical collapse, numerical relativity

(Some figures may appear in colour only in the online journal)

1. Introduction

Energy is a key subject in physics. Due to the equivalence principle, one cannot define the gravitational energy locally. The success of the proof for the positive energy theorem inspired people to define the gravitational energy at the quasi-local level: the energy contained in a closed two-dimensional surface. Several notions of the quasi-local energy have been constructed, such as the Misner–Sharp energy [1], Brown–York energy [2], Hawking energy [3], Hayward energy [4], and Wang–Yau energy [5, 6]. The descriptions for the energy of gravitational waves were studied in [7–9]. More details can be found in review [10].

By fine-tuning the initial data of a spherically scalar field, Choptuik discovered the critical phenomena in gravitational collapse [11]. On the sub-critical side, the collapse will lead to dispersion, while on the super-critical side, a tiny black hole will form. The critical collapse solution is discretely self-similar along the ever-decreasing time and space scales. This feature is universal, independent of the initial profiles of the matter field. The mass of the tiny black hole forming in the super-critical circumstance satisfies a power law, $M_{BH} \propto |p - p^*|^\gamma$, where p^* is a critical parameter value in the initial data of the scalar field, and $\gamma \approx 0.37$. Critical phenomena in many other collapse models were also observed (see [12] for review). Recently, the critical behavior in 3D gravitational collapse with no symmetry assumptions was studied in [13]. Critical collapse of electromagnetic waves in axisymmetry was investigated in [14, 15]. Novel dynamical critical phenomena in the process of the nonlinear accretion of the scalar field into black holes were observed in [16]. With one typical log-periodic formula in the discrete scale invariance systems, one approximate analytic solution for the spacetime near the center was obtained in [17].

Three versions of the quasi-local energy in the Oppenheimer–Snyder dust collapse model were analyzed in [18]. Quasi-local energy was calculated in the contexts of black hole physics and cosmology in [19–21]. In [22], the gravitational and material energies in a static spherical star were discussed. Considering the fundamental role that energy has been playing in physics, in this paper, we investigate the energy issue in critical collapse, and we are especially interested in the comparison between the contributions from the gravitational and material energies.

This paper is organized as follows. In section 2, we describe the methodology, including the collapse model and the definitions of energy. In section 3, we discuss the energy issue in critical collapse. Some features of the quantity m/r are studied in section 4. In section 5, the results are summarized.

* Author to whom any correspondence should be addressed.

2. Methodology

2.1. Gravitational collapse

We consider the critical collapse of a spherically symmetric massless scalar field ϕ. The action for the system is

$$S = \int \mathrm{d}^4x\sqrt{-g}\left(\frac{R}{16\pi G} - \frac{1}{2}\nabla^\mu\phi\nabla_\mu\phi\right). \tag{1}$$

We set $G = 1$. The corresponding energy-momentum tensor for ϕ is

$$T_{\mu\nu} = \phi_{,\mu}\phi_{,\nu} - \frac{1}{2}g_{\mu\nu}g^{\alpha\beta}\phi_{,\alpha}\phi_{,\beta}. \tag{2}$$

We simulate critical collapse in the polar coordinates,

$$\mathrm{d}s^2 = -A(r,\,t)\mathrm{e}^{-2\delta(r,t)}\mathrm{d}t^2 + \frac{1}{A(r,\,t)}\mathrm{d}r^2 + r^2\mathrm{d}\Omega^2. \tag{3}$$

For the metric (3), some components of the Einstein tensor and the energy-momentum tensor for ϕ are

$$G^t_t = \frac{1}{r^2}(rA_{,r} - 1 + A), \tag{4}$$

$$G^r_r = -\frac{1}{r^2}(-rA_{,r} + 2rA\delta_{,r} + 1 - A), \tag{5}$$

$$G^r_t = -\frac{1}{r}A_{,t}, \tag{6}$$

$$T^t_t = -T^r_r = -\frac{1}{2}A(P^2 + Q^2), \tag{7}$$

$$T^r_t = A\phi_{,r}\phi_{,t}. \tag{8}$$

Define

$$Q(r,\,t) \equiv \phi_{,r}, \quad P(r,\,t) \equiv A^{-1}\mathrm{e}^{\delta}\phi_{,t}. \tag{9}$$

Then the equation $G^t_t = 8\pi T^t_t$ yields

$$A_{,r} = \frac{1 - A}{r} - 4\pi rA(P^2 + Q^2). \tag{10}$$

Using $G^r_r = 8\pi T^r_r$ and equation (10), we obtain

$$\delta_{,r} = -4\pi r(P^2 + Q^2). \tag{11}$$

With $G^r_t = 8\pi T^r_t$, we have

$$A_{,t} = -8\pi rA^2\mathrm{e}^{-\delta}PQ. \tag{12}$$

With equation (9), one obtains

$$Q_{,t} = (A\mathrm{e}^{-\delta}P)_{,r}. \tag{13}$$

For the metric (3), the conservation of the energy-momentum tensor, $T^{\mu\nu}_{;\mu} = 0$, leads to

$$P_{,t} = \frac{1}{r^2}(r^2A\mathrm{e}^{-\delta}Q)_{,r}. \tag{14}$$

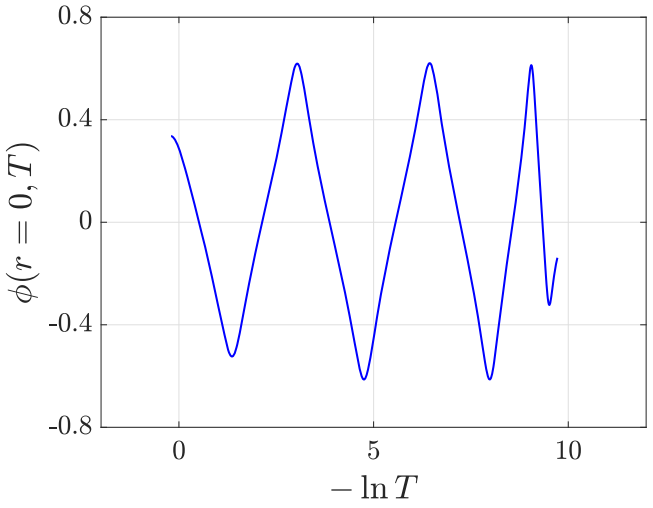

Figure 1. Evolution of the scalar field at the center in critical collapse.

The initial conditions for ϕ are set up as $\phi|_{t=0} = a\exp[-(r/\sigma)^2]$, and $\phi_{,t}|_{t=0} = 0$. The spacial range is $0 \leqslant r \leqslant 12$. In seeking the numerical solution to critical collapse, we set $a = 0.336033778324$ and $\sigma = 1$. The initial values for the metric functions A and δ are obtained via integrations of equations (10) and (11). The regularity of equation (10) at the center requires that $A|_{r=0} = 1$. We choose $\delta|_{r=0} = 0$. Consequently, the coordinate time is equal to the proper time at the center.

In the simulation, we integrate equations (10)–(14) by the fourth-order Runge–Kutta method. Mesh refinement algorithm is implemented. For details on the numerics, see [23].

2.2. Landau–Lifshitz pseudotensor approach

We implement two separate approaches to define the gravitational and material energies: the Landau–Lifshitz pseudotensor approach and the Misner–Sharp energy approach. The Landau–Lifshitz pseudotensor is a typical definition for the energy of the gravitational field and is coordinate-dependent. The Misner–Sharp energy is one of the major notions for the quasi-local energy enclosed in a two-dimensional spacelike surface in spherical symmetry and is coordinate-independent.

Regarding the first approach, we firstly take the following definitions [24, 25],

$$\mathfrak{g}^{\alpha\beta} \equiv \sqrt{-g}\,g^{\alpha\beta}, \tag{15}$$

$$H^{\mu\alpha\nu\beta} \equiv \mathfrak{g}^{\mu\nu}\mathfrak{g}^{\alpha\beta} - \mathfrak{g}^{\mu\beta}\mathfrak{g}^{\alpha\nu}, \tag{16}$$

$$\begin{aligned}(-g)t^{\alpha\beta}_{LL} \equiv \frac{1}{16\pi}\{&\partial_\lambda\mathfrak{g}^{\alpha\beta}\partial_\mu\mathfrak{g}^{\lambda\mu} - \partial_\lambda\mathfrak{g}^{\alpha\lambda}\partial_\mu\mathfrak{g}^{\beta\mu}\\ &+\frac{1}{2}g^{\alpha\beta}g_{\lambda\mu}\partial_\rho\mathfrak{g}^{\lambda\nu}\partial_\nu\mathfrak{g}^{\mu\rho} - g^{\alpha\lambda}g_{\mu\nu}\partial_\rho\mathfrak{g}^{\beta\nu}\partial_\lambda\mathfrak{g}^{\mu\rho}\\ &-g^{\beta\lambda}g_{\mu\nu}\partial_\rho\mathfrak{g}^{\alpha\nu}\partial_\lambda\mathfrak{g}^{\mu\rho} + g_{\lambda\mu}g^{\nu\rho}\partial_\nu\mathfrak{g}^{\alpha\lambda}\partial_\rho\mathfrak{g}^{\beta\mu}\\ &+\frac{1}{8}(2g^{\alpha\lambda}g^{\beta\mu} - g^{\alpha\beta}g^{\lambda\mu})(2g_{\nu\rho}g_{\sigma\tau} - g_{\rho\sigma}g_{\nu\tau})\partial_\lambda\mathfrak{g}^{\nu\tau}\partial_\mu\mathfrak{g}^{\rho\sigma}\Big\},\end{aligned} \tag{17}$$

where g is the metric determinant, and $t^{\alpha\beta}_{LL}$ is called the Landau–Lifshitz pseudotensor. The tensor density $H^{\alpha\mu\beta\nu}$

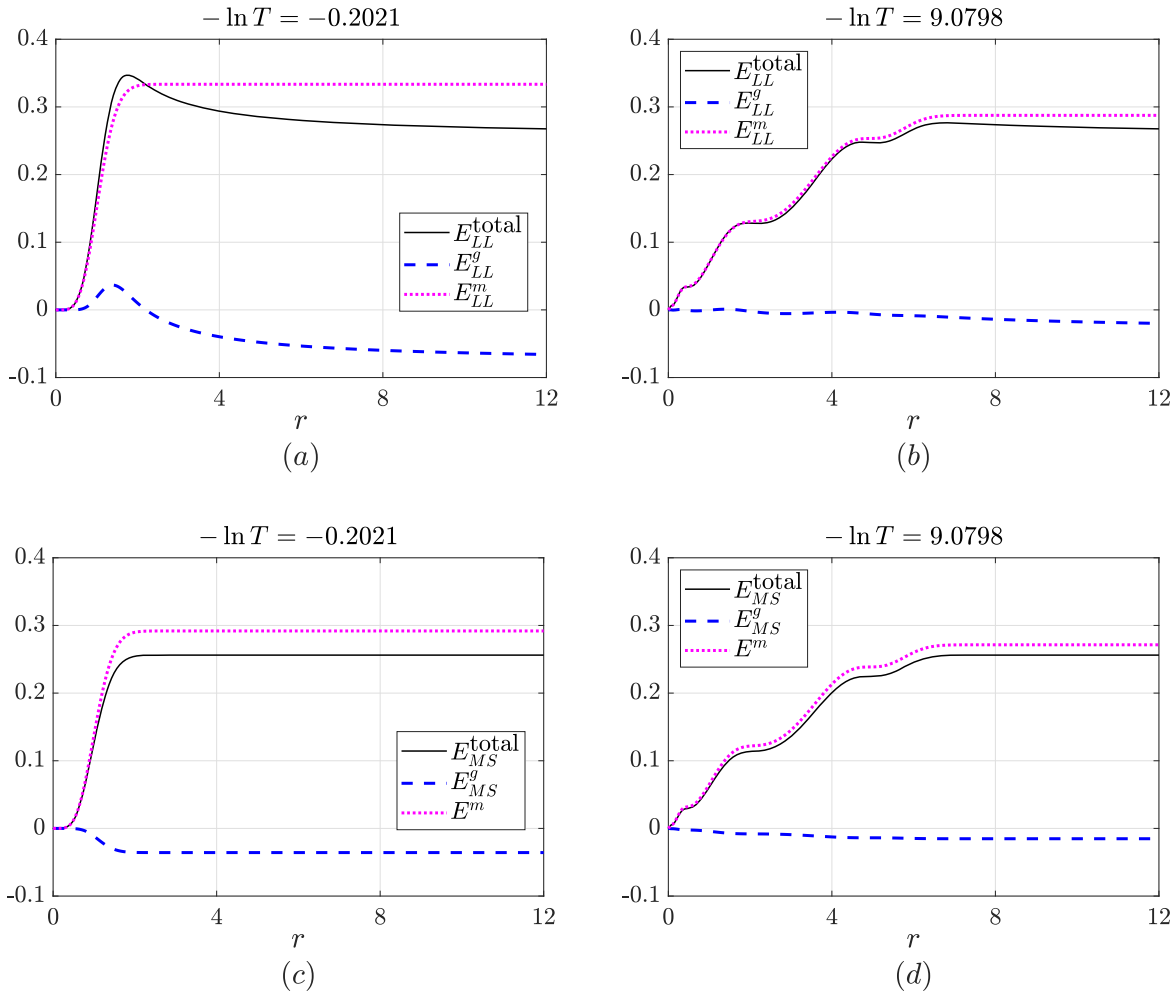

Figure 2. Gravitational and material energies in critical collapse defined by equations (21), (25), (26), (30)–(32).

satisfies the identity

$$\partial_{\mu\nu}H^{\alpha\mu\beta\nu} = 2(-g)G^{\alpha\beta} + 16\pi(-g)t_{LL}^{\alpha\beta}. \tag{18}$$

Then the Einstein equations can be expressed in the non-tensorial form

$$\partial_{\mu\nu}H^{\alpha\mu\beta\nu} = 16\pi(-g)(T^{\alpha\beta} + t_{LL}^{\alpha\beta}). \tag{19}$$

Using the antisymmetric property of $H^{\mu\alpha\nu\beta}$ and the Einstein field equations, one obtains

$$\partial_{\beta}[(-g)(T^{\alpha\beta} + t_{LL}^{\alpha\beta})] = 0. \tag{20}$$

Equations (19) and (20) imply that $t_{LL}^{\alpha\beta}$ can be interpreted as an energy-momentum (pseudo) tensor for the gravitational field.

The quantity $t_{LL}^{\alpha\beta}$ is nontensorial and is usually considered to be meaningless. However, the nontensorial nature of an object does not imply that it is meaningless. The Christoffel symboles are nontensorial. However, they do have geometric and physical content. Although these coefficients can be taken to be zero at a given point by coordinate transformation, they cannot be transformed to zero on an open domain in curved spacetime [10]. Consequently, we think that $t_{LL}^{\alpha\beta}$ may carry some useful information.

We define a total energy associated with the region V,

$$E_{LL}(V) \equiv \int_V (-g)(T^{00} + t_{LL}^{00})\mathrm{d}^3x. \tag{21}$$

When V includes the whole space, $E_{LL}(V)$ coincides with the Arnowitt–Deser–Misner mass. Since the value of the pseudotensor is coordinate-dependent, we choose the coordinates carefully when using a pseudotensor. Here we prefer the Cartesian coordinates, in which for the metric (3), there are

$$g_{tt} = -A\mathrm{e}^{-2\delta}, \qquad g_{ij} = \delta_{ij} + \frac{x_i x_j(1-A)}{r^2 A}. \tag{22}$$

Substitution of equation (22) into (21) yields

$$E_{LL}(V) = \frac{r}{2}\left(\frac{1}{A} - 1\right). \tag{23}$$

Substituting equation (22) into (17) and using $g \equiv |g_{\mu\nu}| = -\mathrm{e}^{-2\delta}$, we obtain

$$(-g)t_{LL}^{00} = \frac{(A-1)A_{,r}}{8\pi r A^2}. \tag{24}$$

With equation (2), we have $T^{00} = (1/2)\mathrm{e}^{-2\delta}(P^2 + Q^2)$. Then we can split the total energy (21) into the material and

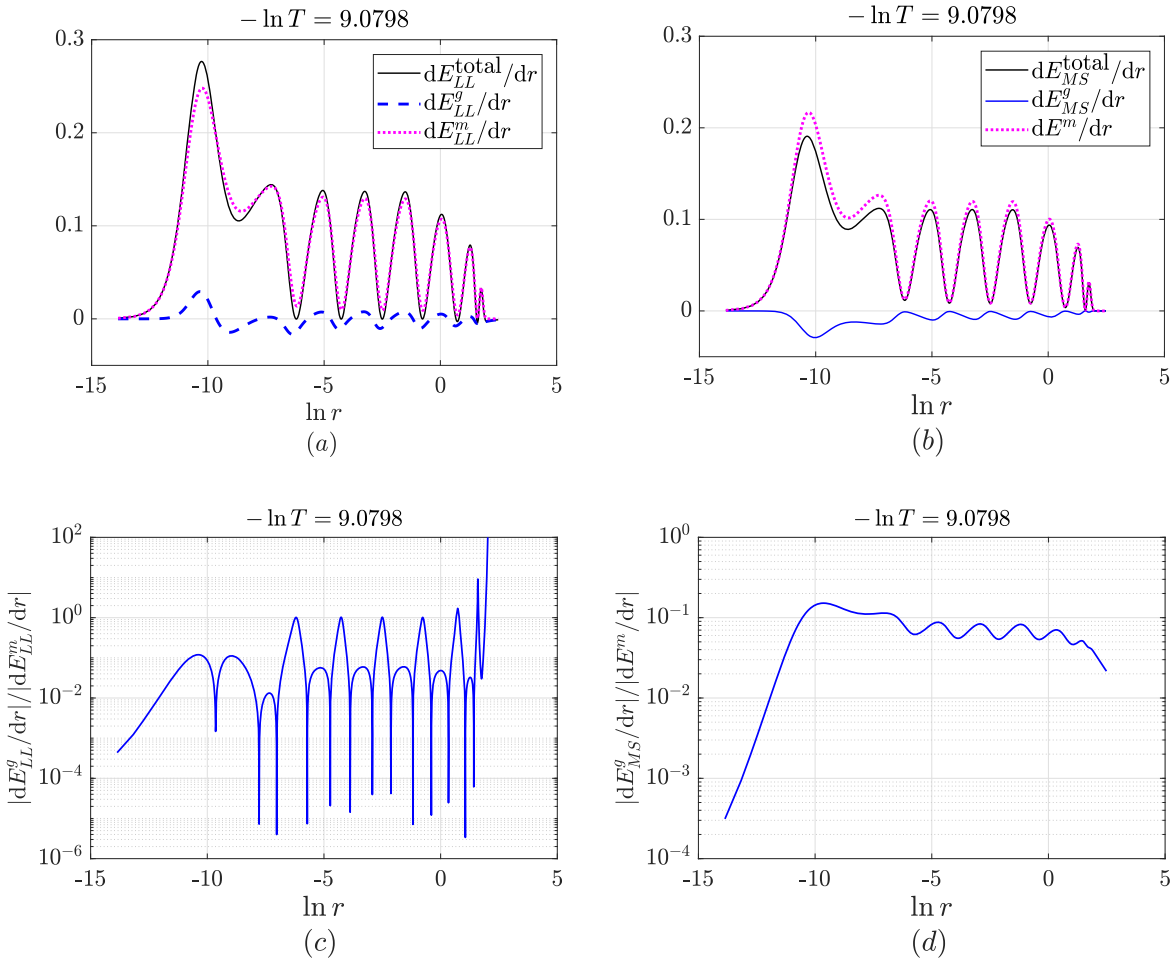

Figure 3. Energy density at the critical collapse stage. The absolute value of the ratio between the gravitational and material energy densities in the large-radius region is much greater than that in the small-radius one.

gravitational parts,

$$E^{m}_{LL}(V) \equiv \int_V (-g)T^{00}\mathrm{d}^3x = 4\pi\int_0^r \frac{1}{2}(P^2+Q^2)r^2\mathrm{d}r, \tag{25}$$

$$E^{g}_{LL}(V) \equiv \int_V (-g)t^{00}_{LL}\mathrm{d}^3x = 4\pi\int_0^r \frac{(A-1)A_{,r}}{8\pi rA^2}r^2\mathrm{d}r. \tag{26}$$

2.3. Misner–Sharp energy approach

Before discussing the definitions for the material and gravitational energies in critical collapse with the Misner–Sharp energy approach, we first consider the energy issue in a static star of perfect fluid, with the energy-momentum tensor, $T_{\mu\nu}=(\rho_f+p_f)U_\mu U_\nu+p_f g_{\mu\nu}$, where U^μ is the tangent vector of the stationary observer. Inside the star, one mass function can be defined as

$$m(r) \equiv 4\pi\int_0^r \rho_f r'^2\mathrm{d}r' = \frac{r}{2}(1-g^{-1}_{rr}). \tag{27}$$

On the boundary of the star $r=r_b$, there is

$$M = m(r_b) = 4\pi\int_0^{r_b}\rho_f r'^2\mathrm{d}r', \tag{28}$$

which is identical to the expression for the total mass in Newtonian gravity. However, in general relativity, the proper mass is

$$M_p = \int \rho_f\sqrt{h}\,\mathrm{d}r'\wedge\mathrm{d}\theta\wedge\mathrm{d}\phi = 4\pi\int_0^{r_b}\rho_f A^{-1/2}r'^2\mathrm{d}r', \tag{29}$$

where $h(=A^{-1}r'^4\sin^2\theta)$ is the determinant of the induced metric $h_{ab}[=\mathrm{diag}(A^{-1}, r'^2, r'^2\sin^2\theta)]$ of the spacelike hypersurface $t=\mathrm{Const}$.

The quantity M in equation (28) has clear physical meaning: it is the total mass (energy) of the Schwarzschild spacetime, including gravitational potential energy. However, the quantity M_p in equation (29) does not include gravitational potential energy, since ρ_f (the energy density measured by a stationary observer) includes the rest energy density of each particle in the star and the internal energy density, but does not include the gravitational energy density [22].

Regarding the Misner–Sharp energy approach of defining the material and gravitational energies in critical collapse, we take similar method as in the static circumstance discussed above. We use the Misner–Sharp energy [1] to represent the total energy inside a closed two-dimensional spacelike surface

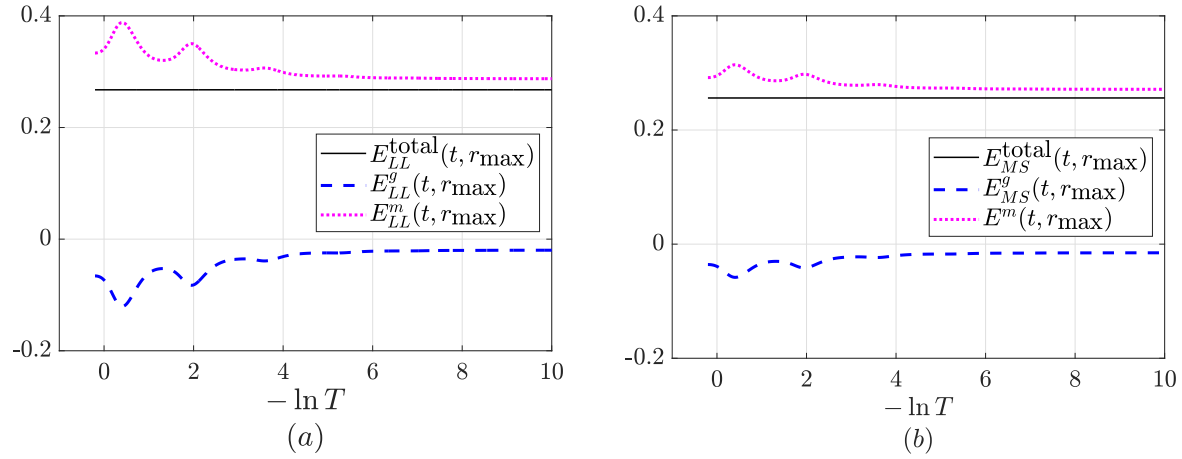

Figure 4. Evolution of the energy inside the region $r \leqslant 12$.

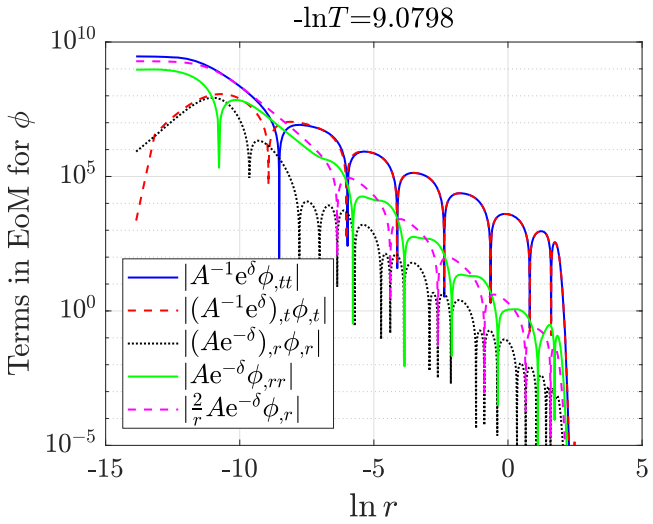

Figure 5. Terms in the equation of motion for ϕ (14). In the small and large-radius regions, equation (14) is respectively reduced to $\phi_{,tt} \approx r^{-2}(r^2\phi_{,r})_{,r}$ and $A^{-1}{\rm e}^{\delta}\phi_{,tt} \approx -(A^{-1}{\rm e}^{\delta})_{,t}\phi_{,t}$.

S constrained by $r = {\rm Const}$ and $t = {\rm Const}$.

$$\begin{aligned} E^{\rm total}_{MS}(r) &\equiv \frac{r}{2}(1 - g^{\mu\nu}r_{,\mu}r_{,\nu}) \\ &= \frac{r}{2}(1 - A) \\ &= 4\pi\int_0^r \rho r'^2 {\rm d}r' \\ &= 4\pi\int_0^r \frac{1}{2}A(P^2+Q^2)r'^2{\rm d}r', \end{aligned} \tag{30}$$

where ρ is the material energy density measured by a stationary observer, $\rho \equiv T_{\mu\nu}U^{\mu}U^{\nu} = (1/2)A(P^2+Q^2)$. U^{μ} is the tangent vector of the stationary observer, $U^{\mu} = (\sqrt{-g^{tt}}, 0, 0, 0)$. The material and gravitational energies are respectively defined as below,

$$\begin{aligned} E^{m} &\equiv \int \rho\sqrt{h}\,{\rm d}r' \wedge {\rm d}\theta \wedge {\rm d}\phi \\ &= 4\pi\int_0^r \frac{1}{2}\sqrt{A}\,(P^2+Q^2)r'^2{\rm d}r', \end{aligned} \tag{31}$$

$$E^{g}_{MS} \equiv E^{\rm total}_{MS} - E^{m} = 4\pi\int_0^r \frac{1}{2}(A - \sqrt{A}\,)(P^2+Q^2)r'^2{\rm d}r'. \tag{32}$$

3. Results I: energy

By fine-tuning the initial data of the scalar field, we obtain the numerical solution to critical collapse. The oscillating behavior of the scalar field at the center, ϕ versus $-\ln T$, is shown in figure 1, where $T \equiv t_* - t$, and t_* is the time for naked singularity formation. The period Δ for the oscillations takes the same value as reported in the literature, $\Delta \approx 3.43$.

With the expressions (21), (25), (26), (30)–(32), we plot the material and gravitational energies and energy densities in figures 2 and 3, respectively. We also plot the evolution of the energies in a sufficiently large region of $r \leqslant 12$ in figure 4, such that during the simulation the boundary is far enough from the collapse region and the total energy in the region remains constant. From these figures, we observe that both the Landau–Lifshitz pseudotensor approach and Misner–Sharp energy approach generate similar results:

(i) In critical collapse, the contribution from the material energy is greater than that from the gravitational energy.
(ii) The material energy density, ${\rm d}E^{m}_{LL}/{\rm d}r$ in figure 3(a) and ${\rm d}E^{m}/{\rm d}r$ in figure 3(b), is positive.
(iii) As shown in figure 3(a), the gravitational energy density ${\rm d}E^{g}_{LL}/{\rm d}r$ by the Landau–Lifshitz pseudotensor approach is sometimes negative and sometimes positive. As shown in figure 3(b), the gravitational energy density ${\rm d}E^{g}_{MS}/{\rm d}r$ by the Misner–Sharp energy approach is always negative.

There is a strong correlation between the gravitational effects on the evolution of the scalar field and the ratio between the gravitational and material energy densities. As shown in figure 5, in the large-radius region ($\ln r > -7$), the equation of motion for ϕ (14) is reduced to

$$A^{-1}{\rm e}^{\delta}\phi_{,tt} \approx -(A^{-1}{\rm e}^{\delta})_{,t}\phi_{,t}. \tag{33}$$

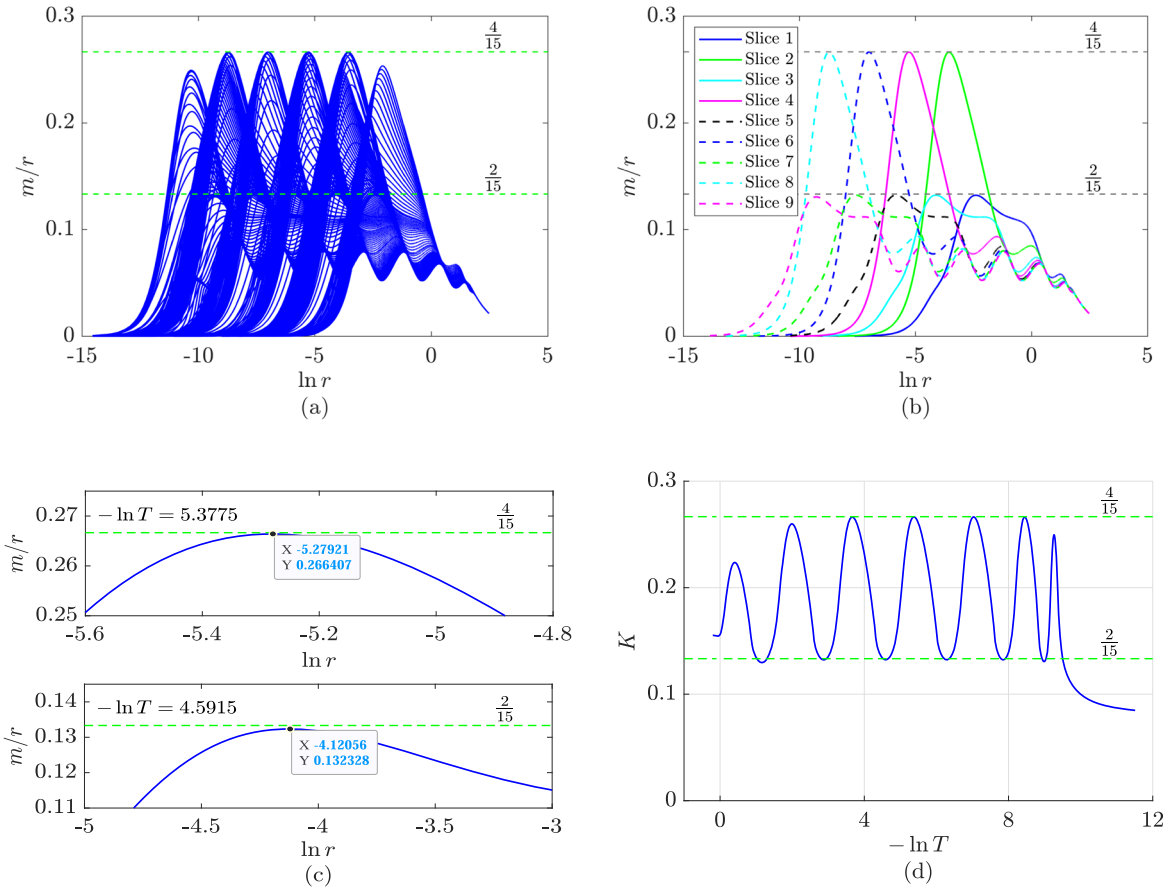

Figure 6. m/r in critical collapse in the polar coordinates (3). (a) and (b): m/r on some slices $t = \text{Const}$. In the transition place between the small- and large-radius regions, the maximum values of m/r stay in the range of $[2/15, 4/15]$. In figure (b), the slices are numbered in the temporal direction. (c) Numerical illustrations on the upper and lower limits for the maximum values of m/r. (d) K: the maximum value of m/r on slices $T = \text{Const}$.

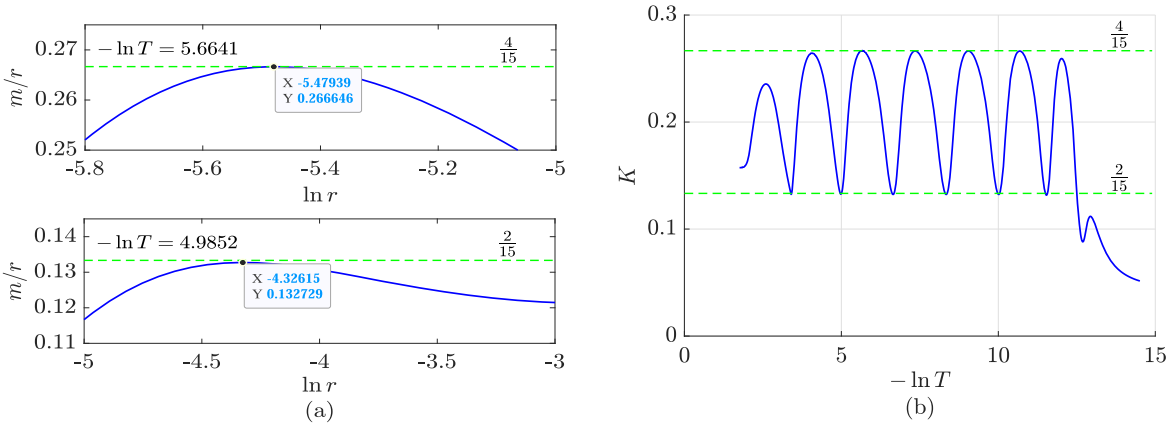

Figure 7. m/r in critical collapse on some slices $t = \text{Const}$ in the double-null coordinates (38). (a) Numerical illustrations on the upper and lower limits for the maximum values of m/r. (b) K: the maximum value of m/r on slices $T = \text{Const}$.

Therefore, the gravitational effects on the dynamics of the scalar field are important. On the other hand, in the small-radius region ($\ln r < -11$), equation (14) becomes

$$\phi_{,tt} \approx r^{-2}(r^2\phi_{,r})_{,r}, \tag{34}$$

which is similar to what happens in flat spacetime. So the scalar field does not feel the gravitational effects directly. On the other hand, as shown in figure 5, in the transition region locating between the central and large-radius ones, in the equation of motion for the scalar field, the gravitational effects are not negligible. Then due to the connection between the central and transition regions, the scalar field in the central region feels the gravitational effects indirectly. Correspondingly, as shown in figure 3, the absolute value of the ratio between the gravitational and material energy densities in the large-radius region is much greater than in the small-radius

one. The echoing behavior of the energy density is clearly demonstrated in figure 3.

We make some comments on the result (34). In another two types of collapse (dispersion and early stage of collapse toward black hole formation), near the center, equation (14) is also reduced to the form (34). The causes are the following. In equation (14), the gravitational effects come from the first-order derivatives of the metric functions. Under the smoothness requirement in the central region, the metric functions and the scalar field have the following asymptotic expressions [23]:

$$A \approx 1 + A_2(t)r^2, \quad \delta \approx \delta_2(t)r^2, \quad \phi \approx \phi_0 + \phi_2(t)r^2.$$

Some details on the analytic investigations of equations (33) and (34) are presented in [26].

As discussed in [26], in the large-radius region, the field ϕ admits the following approximate expression:

$$\begin{aligned}\phi(r, \xi) \approx\ & C_1(1 + C_2[H(r, \xi)]) \\ & \times \cos(\omega \ln r + C_3[H(r, \xi)] + \varphi_0),\end{aligned} \tag{35}$$

where $\xi \equiv t - t_*$, such that $\xi = 0$ upon naked singularity formation. The quantity $[H(r, \xi)]$ has the following features:

(i) For $[H(r, \xi)]$, there is

$$[H(r, \xi)] = H(r, \xi) \equiv \frac{\omega\alpha\xi}{r} = \omega A^{1/2}\mathrm{e}^{-\delta}\frac{\xi}{r}, \tag{36}$$

where $\alpha \equiv A^{1/2}\mathrm{e}^{-\delta}$.

(ii) Note that $H_{,\xi} = \omega\alpha/r + \omega\alpha_{,\xi}\xi/r$. The numerical results yield

$$[H]_{,\xi} \approx \frac{\omega\alpha}{r}, \quad [H]_{,\xi\xi} \approx \frac{\omega\alpha_{,\xi}}{r} \approx -\delta_{,\xi}[H]_{,\xi}. \tag{37}$$

The numerical results show that the transition region located between the central and large-radius regions can be described as $r \in [r_1,\ r_2]$. At $r = r_1$, there is $|C_3H| \sim |\omega \ln r|$; and at $r = r_2$, there is $|C_3H_{,r}| \sim \omega/r$.

4. Result II: *m*/*r*

In gravitational collapse, m/r is an important quantity identifying the location of the apparent horizon, which is also crucial in identifying the formation of singularities [27], where m is the Misner–Sharp mass. It is natural to ask how far the spacetime in critical collapse is from black hole formation. Moreover, as studied in [28], the quantity m/r is closely related to the origin of the characteristic period in critical collapse $\Delta \approx 3.43$.

We plot the evolution of m/r on some slices $t = \mathrm{Const}$ in figure 6. On each slice $t = \mathrm{Const}$, the quantity m/r takes its maximum value, denoted as $(m/r)|_{\max}$, in the transition place between the small- and large-radius regions. In [29], it was reported that the maximum value of $(m/r)|_{\max}$ is 0.26. In this work, we obtain more accurate results. Denote $K(T)$ as the maximum value of m/r on slices $T = \mathrm{Const}$. As shown in figure 6, the numerical results for the upper and lower limits for K are about 0.266 407 and 0.132 328, respectively. With the same code used in [30], we simulate critical collapse in the double-null coordinates,

$$\begin{aligned}\mathrm{d}s^2 &= -4\mathrm{e}^{-2\sigma(u,v)}\mathrm{d}u\mathrm{d}v + r^2(u, v)\mathrm{d}\Omega^2 \\ &= \mathrm{e}^{-2\sigma(t,x)}(-\mathrm{d}t^2 + \mathrm{d}x^2) + r^2(t, x)\mathrm{d}\Omega^2,\end{aligned} \tag{38}$$

where $u = (t - x)/2$ and $v = (t + x)/2$. As shown in figure 7, we obtain the numerical results for the upper and lower limits for K which are 0.266 646 and 0.132 729, respectively. So it is natural to state the limits by the fractional numbers, $4/15$ and $2/15$.

There is a big gap between the upper limit for m/r in critical collapse (which is $4/15$) and the criterion for black hole formation (which is $m/r = 1/2$). This is reasonable since dispersion, critical collapse and black hole formation are three distinct final outcomes of gravitational collapse.

5. Summary

Energy has played a fundamental role in physics, and the explorations on this concept keep bringing us an insightful understanding of nature. However, in general relativity, because of the nontensorial characteristic of the gravitational energy-momentum density expression, the energy issue in gravitational collapse has not been fully studied in the literature. A nontensorial object may still be meaningful. The Christoffel symbols are nontensorial and one can make them to be zero at a given point by coordinate transformation. However, they cannot be transformed to zero on an open domain in curved spacetime. So in this paper we took the adventure of studying the energy issue in critical collapse with the Landau–Lifshitz pseudotensor approach and Misner–Sharp energy approach. These two approaches generate similar results: in critical collapse, the contribution from the material energy is greater than that from the gravitational energy.

The quantity m/r is indispensable in identifying the formation of the apparent horizon in gravitational collapse. In this paper, it was observed that in critical collapse the maximum value of m/r fluctuates between $2/15$ and $4/15$. So the upper bound $4/15$ for m/r is a bit far from the criterion for black hole formation, $m/r = 1/2$.

Acknowledgments

The authors are very grateful to the anonymous referees for their valuable comments. The authors thank Xiaokai He, Xiaoning Wu, and Cheng-Yong Zhang for the helpful discussions. YH and CGS are supported by the National Natural Science Foundation of China (Grant No. 11925503). JQG is supported by Shandong Province Natural Science Foundation under grant No.ZR2019MA068.

ORCID iDs

Jun-Qi Guo https://orcid.org/0000-0002-3280-0163

References

[1] Misner C W and Sharp D H 1964 Relativistic equations for adiabatic, spherically symmetric gravitational collapse *Phys. Rev.* **136** B571

[2] Brown J D and York J W Jr 1993 Quasilocal energy and conserved charges derived from the gravitational action *Phys. Rev.* D **47** 1407

[3] Hawking S W 1968 Gravitational radiation in an expanding universe *J. Math. Phys.* **9** 598

[4] Hayward S A 1994 Quasilocal gravitational energy *Phys. Rev.* D **49** 831

[5] Wang M-T and Yau S-T 2009 Quasilocal mass in general relativity *Phys. Rev. Lett.* **102** 021101

[6] Wang M-T and Yau S-T 2009 Isometric embeddings into the Minkowski space and new quasi-local mass *Commun. Math. Phys.* **288** 919

[7] Isaacson R A 1968 Gravitational radiation in the limit of high frequency: I. the linear approximation and geometrical optics *Phys. Rev.* **166** 1263

[8] Isaacson R A 1968 Gravitational radiation in the limit of high frequency: II. Nonlinear terms and the effective stress tensor *Phys. Rev.* **166** 1272

[9] Cai R-G, Yang X-Y and Zhao L 2022 On the energy of gravitational waves *Gen. Relativ. Gravit.* **54** 89

[10] Szabados L B 2009 Quasi-local energy-momentum and angular momentum in general relativity *Living Rev. Relativ.* **12** 1

[11] Choptuik M W 1993 Universality and scaling in gravitational collapse of a massless scalar field *Phys. Rev. Lett.* **70** 9

[12] Gundlach C and Martin-Garcia J M 2007 Critical phenomena in gravitational collapse *Living Rev. Relativ.* **10** 1

[13] Deppe N, Kidder L E, Scheel M A and Teukolsky S A 2019 Critical behavior in 3D gravitational collapse of massless scalar fields *Phys. Rev.* D **99** 024018

[14] Baumgarte T W, Gundlach C and Hilditch D 2019 Critical phenomena in the gravitational collapse of electromagnetic waves *Phys. Rev.* D **123** 171103

[15] Mendoza M F P and Baumgarte T W 2021 Critical phenomena in the gravitational collapse of electromagnetic dipole and quadrupole waves *Phys. Rev.* D **103** 124048

[16] Zhang C-Y, Chen Q, Liu Y, Luo W-K, Tian Y and Wang B 2022 Critical phenomena in dynamical scalarization of charged black holes *Phys. Rev. Lett.* **128** 161105

[17] Guo J-Q and Zhang H 2019 Geometric properties of critical collapse *Eur. Phys. J.* C **79** 625

[18] He X-K and Xie N-Q 2020 Quasi-local energy and Oppenheimer-Snyder collapse *Class. Quantum Grav.* **37** 185016

[19] Afshar M M 2009 Quasilocal energy in FRW cosmology *Class. Quantum Grav.* **26** 225005

[20] Miller W A, Ray S, Wang M-T and Yau S-T 2018 Wang and Yau's quasi-local energy for an extreme Kerr spacetime *Class. Quantum Grav.* **35** 055007

[21] Gudapati N and Yau S-T 2021 Quasi-local mass near the singularity, the event horizon and the null infinity of black hole spacetimes *Adv. Theor. Math. Phys.* **25** 101

[22] Liang C B and Zhou B 2006 *Introduction to Differential Geometry and General Relativity* (Beijing: Science Press) vol 1

[23] Zhang C-Y, Tang Z-Y and Wang B 2016 Gravitational collapse of massless scalar field in $f(R)$ gravity *Phys. Rev.* D **94** 104013

[24] Landau L D and Lifshitz E M 1971 *The Classical Theory of Fields* (Pergamon Press) Course of Theoretical Physics Series vol 2

[25] Poisson E and Will C 2014 *Gravity* (Cambridge University Press)

[26] Guo J-Q, Hu Y, Wang P-P and Shao C-G New results on the dynamics of critical collapse arXiv:2307.04372 [gr-qc]

[27] Zhang C-Y, Tang Z-Y and Wang B 1993 Bounded variation solutions of the spherically symmetric einstein-scalar field equations *Commun. Pure Appl. Math.* **46** 1131

[28] Price R H and Pullin J 1996 Analytic approximations to the space-time of a critical gravitational collapse *Phys. Rev.* D **54** 3792

[29] Choptuik M W 1993 Critical behaviour in scalar field collapse *Proc. of a NATO Advanced Research Workshop on Deterministic Chaos in General Relativity* ed D Hobill, A Burd and A Coley (Springer, LLC) pp 155–75

[30] Guo J-Q, Zhang L, Chen Y, Joshi P S and Zhang H 2020 Strength of the naked singularity in critical collapse *Eur. Phys. J.* C **80** 924